AI-Powered Noncontact In-Home Gait Monitoring and Activity Recognition System Based on mm-Wave FMCW Radar and Cloud Computing

Hajar Abedi, *Graduate Student Member, IEEE*, Ahmad Ansariyan, Plinio P. Morita, *Member, IEEE*, Alexander Wong, *Senior Member, IEEE*, Jennifer Boger, *Member, IEEE*, and George Shaker, *Senior Member, IEEE*

***Abstract*—In this work, we present a cloud-based system for noncontact, real-time recognition, and monitoring of physical activities and walking periods within a domestic environment. The proposed system employs standalone Internet of Things (IoT)-based millimeter wave radar devices and deep learning models to enable autonomous, free-living activity recognition, and gait analysis. To train deep learning models, we utilize range-Doppler maps generated from a data set of real-life in-home activities. The performance of several deep learning models is evaluated based on accuracy and prediction time, with the gated recurrent network [gated recurrent unit (GRU)] model selected for real-time deployment due to its balance of speed and accuracy compared to 2-D convolutional neural network long short-term memory (2D-CNNLSTM) and long short-term memory (LSTM) models. The overall accuracy of the GRU model for classifying in-home physical activities of trained subjects is 93%, with 86% accuracy for a new subject. In addition to recognizing and differentiating various activities and walking periods, the system also records the subject's activity level over time, washroom use frequency, sleep/sedentary/active/out-of-home durations, current state, and gait parameters. Importantly, the system maintains privacy by not requiring the subject to wear or carry any additional devices.**

***Index Terms*—Activity recognition, autonomous systems, gait monitoring, mm-wave radar, sequential deep learning.**

I. Introduction

FEATURES related to gait are fundamental metrics of human motion and human health [1]. Human gait is a valuable and feasible clinical marker to determine the risk of functional decline—both mental and physical [2], [3]. Changes in gait parameters from a person's normal values often indicate deteriorating changes in health [4]. Technologies that detect changes in people's gait patterns, especially older adults, could support the detection, evaluation, and monitoring of parameters related to changes in mobility, cognition, and frailty [5]. Gait assessments could be leveraged as a clinical measurement as they are not limited to a specific healthcare discipline and are consistent and sensitive tests [2]. Numerous studies have been conducted to identify the relative association between walking and functional decline in people, especially older adults (e.g., [6], [7], [8], and [9]). While gait parameters have been assessed and used as a clinical indicator for health status in various studies, there is no consensus for a standard measurement methodology for walking tests [2]. Moreover, most of the measurements are conducted during clinical visits [6]. However, variations in gait characteristics as a result of cognitive or other conditions may go undetected as the effect can be gradual and often goes unnoticed by the individual and/or during clinical visits [10]. Another issue related to assessing gait is that the unfamiliar setting of a clinic often causes people to (intentionally or unintentionally) change their gait patterns during clinical assessments. While systems, such as GaitRite [11] and Vicon [12] are currently available and provide precise measurements of gait, such systems are expensive and difficult to operate, making them impractical for a clinic and not suitable for in-home monitoring. Therefore, there is a pressing need for affordable technology that can measure human gait parameters continuously, unobtrusively, and reliably if we are to get a better understanding of people's true gait and how their gait may change over time. A system is needed to measure and analyze people's gait in their living environment, namely, at home, in hospitals or long-term care facilities.

A wearable device could be a possible solution for frequent in-home gait assessments [13], [14] but using them requires people to want and remember to use and recharge them. Moreover, wearable devices might cause feelings of burden and discomfort. On the other hand, optics-based systems, such as computer vision and infrared, have line-of-sight detection problems (i.e., they cannot detect people behind obstacles), as well as privacy-related issues and overhead costs [12], [15].

Manuscript received 5 October 2021; revised 29 November 2022; accepted 23 December 2022. Date of publication 9 January 2023; date of current version 23 May 2023. This work was supported by in part by NSERC; in part by MITACS; in part by Microsoft Inc.; and in part by Texas Instrument. *(Corresponding author: Hajar Abedi.)*

This work involved human subjects or animals in its research. The authors confirm that all human/animal subject research procedures and protocols are exempt from review board approval.

Hajar Abedi, Alexander Wong, and Jennifer Boger are with the Department of Systems Design Engineering, University of Waterloo, Waterloo, ON N2L 3G1, Canada (e-mail: habedifi@uwaterloo.ca; alexander.wong@uwaterloo.ca; jboger@uwaterloo.ca).

Ahmad Ansariyan and George Shaker are with the Electrical Engineering Department, University of Waterloo, Waterloo, ON N2L 3G1, Canada (e-mail: ahmad.ansariyan@uwaterloo.ca; gshaker@uwaterloo.ca).

Plinio P. Morita is with the School of Public Health Sciences, University of Waterloo, Waterloo, ON N2L 3G1, Canada (e-mail: plinio.morita@uwaterloo.ca).

Digital Object Identifier 10.1109/JIOT.2023.3235268

A wireless technology that uses electromagnetic waves (i.e., radar) to continually measure gait parameters at home, in long-term care or in a hospital, without a clinician's involvement has been proposed as a suitable solution for many of the issues discussed above [10], [16], [17], [18], [19], [20], [21], [22], [23]. The use of a radar system is appealing due to its reliable functionality in different lighting levels, protection of privacy, penetration through obstacles, and long-range detection capabilities [23]. Radar sensors could make it possible to monitor and analyze gait outside the laboratory and capture information about human gait and activity levels during the person's everyday activities [24], [25], [26]. It should be mentioned that there is little research about radar's accuracy and applicability, and people may not feel comfortable installing radars in their homes (since it is new and not a common technology). However, there is growing interest in the use of radar systems in everyday life [15], [27].

Studies on the application of radar technologies in human gait assessment have been conducted to: 1) analyze and obtain gait parameters [10], [16], [17], [18], [19], [20], [21] and 2) recognize humans from their gait patterns citebib28, [29], [30], [31], [32], [33]. For the first one, various radar signal processing methods have been proposed to extract gait characteristics such as speed, cadence, stride length, etc. Machine learning and artificial intelligence (AI) have been deployed for the latter. However, the focus of this article is to integrate machine learning algorithms with radar signal processing to identify the type of in-home activity performed by a subject and to detect in-home walking periods to distinguish them from other in-home activities.

II. State of the Art and Proposed Improvements

Most of the current gait analysis systems are based on continuous-wave (CW) radars; such systems enable Doppler/micro-Doppler measurement but prevent range estimates [29], [34], [35], [36], [37]. As shown in [38], one of the main drawbacks of CW radars is the effects of the approach angles of motion on the micro-Doppler patterns. For instance, a micro-Doppler signature of a person walking toward the radar at a relative 90° angle is different from that at 0° angle [19], [20], [28]. Previous works on developing radar-based gait detection systems have primarily focused on straight-line walking periods to tackle the dependency of micro-Doppler patterns on the angle of motion [19], [20], [26], [28]. However, the chance of in-home straight-line walking is very low as people walk randomly in their living environment. To overcome the dependency of the relative angle, one possible solution is to obtain the walking speed through the changes in a subject's position over time (i.e., velocity = position/time). A multiple inputs multiple outputs (MIMOs) frequency modulated continuous wave (FMCW) radar [23], [33], [39], [40], [41], [42] can provide the position of targets in addition to the micro-Doppler information, which makes it a good candidate for in-home gait monitoring assessment and activity recognition application [10].

Although the speed of random walking could be extracted using an MIMO FMCW radar, the position of a subject performing other in-home nonwalking activities, such as cleaning or working out also changes over time. Therefore, we need an algorithm to distinguish walking periods from other in-home activities and movements for an in-home gait monitoring assessment and activity recognition system. In this article, we propose a novel cloud-based in-home free-living activity recognition and gait monitoring system that integrates radar-based signal processing methods with a sequential deep learning algorithm to create an autonomous in-home gait monitoring and activity recognition (AI-GM&AR) system. Our proposed AI-GM&AR system uses a sequential deep learning model to recognize the type of in-home activity, detect walking periods, and distinguish them from other in-home activities.

The primary purpose of our research is to perform in-home typical daily activity recognition and gait period detection using radar to have a record of the subject's activity level and gait patterns during daily life activities. We perform gait and activity recognition studies in a familiar and commonly used environment, such as one's home.

Most of the research on human gait analysis and activity recognition has been done in a simple, large, and low-clutter environment with a constrained range and limited activity (mainly in a straight line) [20], [23], [28], [39], [43], [44], [45], [46]. However, when someone walks randomly or performs in-home activities in a cluttered environment such as a typical home, their patterns are different from that of straight-line activity in a large area [20], [23], [28], [39], [43]. As will be shown in this article, identifying walking periods and recognizing the type of activity a person performs is complicated in such an environment using radar signal processing methods.

Moreover, short-time Fourier transform (STFT) has been widely used to train machine learning algorithms in many cases [44], [45]. STFT is a good solution for such a straight-line activity where it captures all micro-doppler which depends on relative angle. The reason is that, for a straight-line movement, the relative angle between the radar and the subject is constant, thus, the direction will not impact the extracted micro-Doppler. However, when it comes to random and nonstraight-line in-home activities at various angles, STFT patterns are not easily distinguishable. Since people have different patterns of walking and other in-home activities, as will be shown in this article, if we train a model with STFT, it will not produce the best results. Furthermore, since STFT ignores the spatial information of subjects (e.g., range information), it does not have enough information to distinguish various in-home activities.

Moreover, unlike the work reported in [21] that used a complex radar system including four AWR1243 chips to create 192 channels to provide human point cloud information for 2D-CNN, we used only one AWR1443Boost radar sensor. Note that for a real-time everyday application, we need a fast and simple algorithm, whereas an expensive high-resolution radar and complex signal processing are required to prepare accurate point cloud information, as shown in [21]. Moreover, to make the system affordable, it is preferred to have fewer and less expensive radar sensors. In this article, we show that, without the need for an expensive high-resolution radar

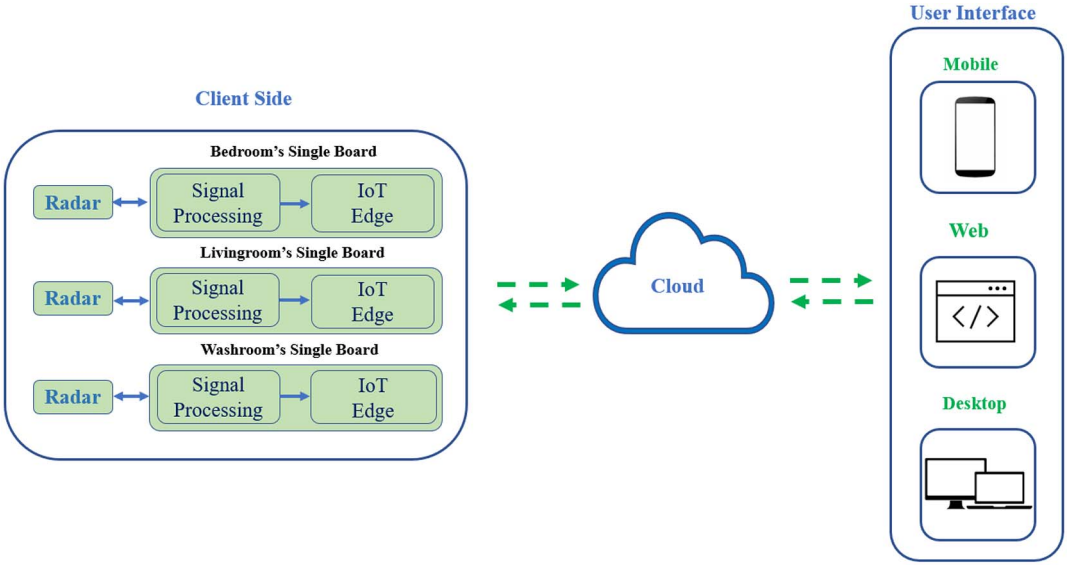

Fig. 1. Diagram of the proposed AI-GM&AR system. Three standalone units are installed in the subject's living environment collecting stream data and sending it to the cloud. In addition to gait parameters and the subject's current status, the subject's daily activity reports are recorded and shown using three different platforms: mobile, Web, and desktop apps.

leading to complicated and computational-costly algorithms for detection, clustering, and associations to extract point cloud information (x–y–z) [21]. A range-Doppler map (RDM) of a human body obtained from a low-cost radar is reliable and provides enough features for our purposes. RDMs are delivered to a sequential deep-learning algorithm to be trained and predict in-home activities. In addition to the simplicity, compared to the point cloud method, another advantage of RDM is that only one single transmitter and a receiver can provide both the occupied position and all created micro-Doppler, leading to a less expensive system. Another advantage of using RDMs is that, compared to SFTF patterns, the RDM has both spatial and temporal features of subjects.

Furthermore, assessing various deep learning models, we show that gated recurrent unit (GRU) [47] can extract temporal characteristics of the radar data and thus achieve sufficient recognition accuracy with relatively low complexity compared to the existing 2D-CNN and 2-D convolutional neural network long short-term memory (2D-CNNLSTM) methods [48]. Since RDM preprocessing is simple and fast, all signal processing pipelines are performed in a low-cost standalone Internet of Things (IoT) Edge device without allocating an extra laptop or PC for signal processing. In this article, we utilize a Raspberry Pi to process radar raw data and perform all signal processing to be delivered to the GRU network. With simple and fast preprocessing to create RDMs performed by a Raspberry Pi, streamed data is sent to the cloud (Microsoft Azure), and the GRU network is applied to the streamed data to identify the type of activity a subject is performing in real time.

Our proposed cloud-based AI-GM&AR system not only detects walking periods and captures gait values but also contains rich information about a person's daily activity level, such as the time the person started and stopped walking, the distance of walking, how long the subject was stationary, how long the subject was active during a day (all other movements in addition to walking), if the target left home, etc. Additionally, the proposed standalone AI-GM&AR system provides a record of the subject's activity level over time, washroom frequency and duration, and sleep/sedentary/active/out-of-home durations accessible in the designed business intelligence dashboard developed in Azure. These daily reports provide the level of activities of daily living used as an indicator of a person's functional status [49]. The reports also could be used to collectively describe that the person has the fundamental skills required to independently care for oneself [50].

III. AI-GM&AR System Design

The diagram of our proposed AI-GM&AR system is presented in Fig. 1. The system's main components include the Client Side, Cloud, and User Interface. To provide a detailed representation of the subject's daily activity, we focus our attention on the living room in this article as this is the central area of the house where the subjects spend most of their time and perform most of their activities, followed by the bedroom (to record sleeping time and duration) and the washroom (to record washroom frequency, enter, exit, and duration). Therefore, to enable tracking a subject in the three main living areas, we installed a standalone system (a radar integrated with a single board) in the subject's bedroom, living room, and washroom. Each system sends the radar configuration commands to run the radar, stores received raw signals, preprocess the raw data, and then transfers it to the cloud. Each system in each room performs a signal processing chain to detect the presence or absence of the subject. To identify which space is currently occupied, a presence-absence detection (PAD) algorithm is applied to the radar raw data [51]. We refer interested readers for more detail on the PAD algorithm to our previous papers published in [49] and [51]. The PAD algorithm identifies the rooms as occupied or vacant. The data from the room occupied by the subject is sent to the

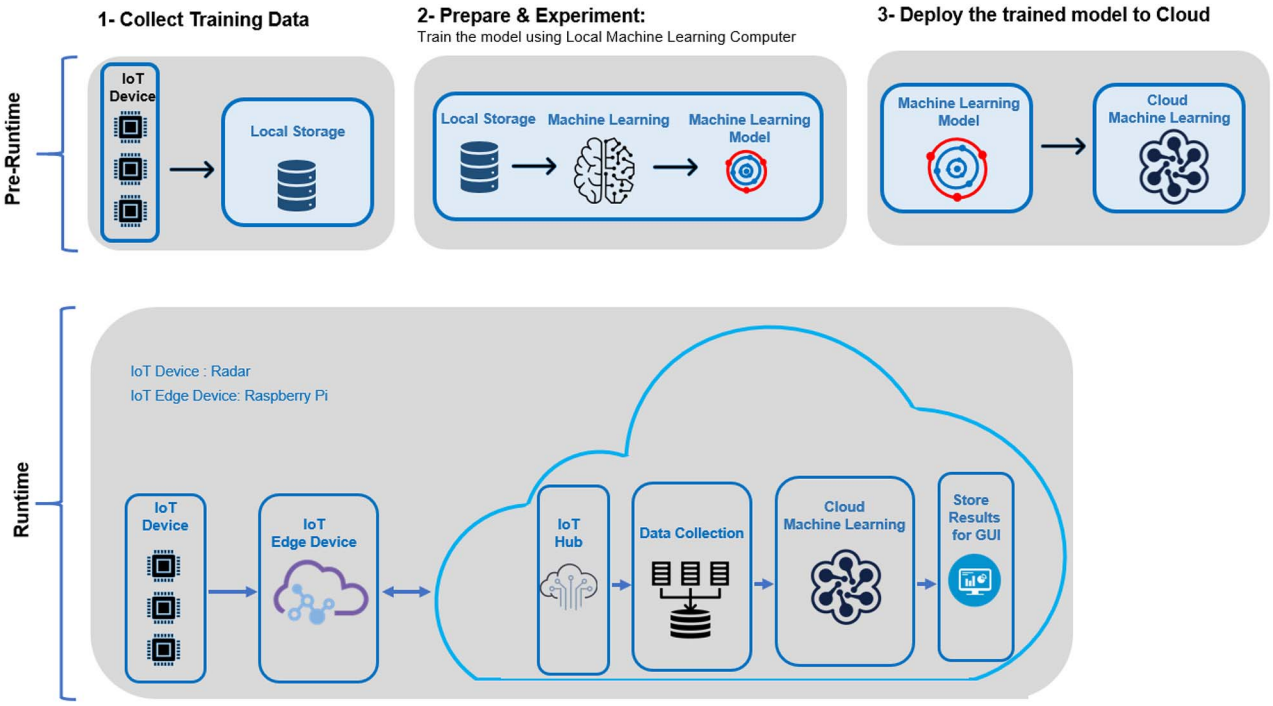

Fig. 2. Flowchart of the IoT-based AI-GM&AR system showing the prerun time and run-time processes in the cloud.

cloud through the IoT Edge. Since our focus is on activity recognition and gait period identification in the living room in this article, if the living room is occupied, then the RDM will be sent to the cloud for further analysis. The pseudo-code of our proposed AI-GM&AR system is provided in Algorithm 1. The radar real-time raw data captured in each room is the system's input to generate the subject's activity report output. If the PAD algorithm identifies the presence of a subject in the bed (occupied bed), the time duration of in-bed status will be stored in the cloud database to record the sleep or in-bed time. On the other hand, if the presence of the subject is identified by the PAD algorithm in the washroom, the entrance/exit time and the time duration the subject spends in the washroom will be recorded. Deploying deep learning in the cloud, the type of activity performed by the subject will be predicted. If the PAD algorithm identifies the absence of the subject in all three areas, the status of the out-of-home will be determined (a vacant room). The time duration the subject spends out of home would also be recorded.

Algorithm 1 In-Home Status Recognition Algorithm

```
Input: Radars Raw Data from each Single Board
Output: Activity Reports
while True:
  chirp=capture_raw_data ()
  room=PAD (chirp)
  if room == "in_bed"
    save_in_bed_date_and_time ()
  else if room="in_washroom"
    save_in_washroom_date_and_time ()
  else if room="out_of_home"
    save_out_of_home_date_time ()
  else if room== "Livingroom"
    status=check_status_of_livingroom (chirp)
      save_status_of_livingroom (status, date, time)
```

A. Deploying Machine Learning in the Cloud

There are two main steps in cloud computing to deploy real-time machine learning [52]: 1) preruntime and 2) run-time processes. As shown in Fig. 2, in the preruntime step, we collect data from the IoT device (the radar sensor) to train a deep learning network. The model is trained and optimized in a local machine. The model is then deployed into the cloud to be used in the run-time section. In the run-time step, radar sensors paired with Raspberry Pis (standalone sensors) are used to capture and preprocess streamed data from the environment and then send it to the cloud for further analysis. If the occupied room is the living room, the stream data is then transferred to the cloud and fed into the deep learning network to identify the type of in-home activity and gait periods [52]. More details are provided in Section IV.

IV. Proposed AI-GM&AR Algorithm

The block diagram of our AI-GM&AR algorithm flowchart is illustrated in Fig. 3. The proposed algorithm consists of two processes: 1) walking period identification and activity recognition and 2) gait parameter extraction. This article covers the method of in-home walking period identification and activity recognition. For gait parameter extraction, we refer interested readers to our previous work done for gait analysis in a cluttered environment [26].

In our proposed system, radar raw data is collected from a MIMO FMCW radar. As shown in Fig. 3 and Algorithm 2,

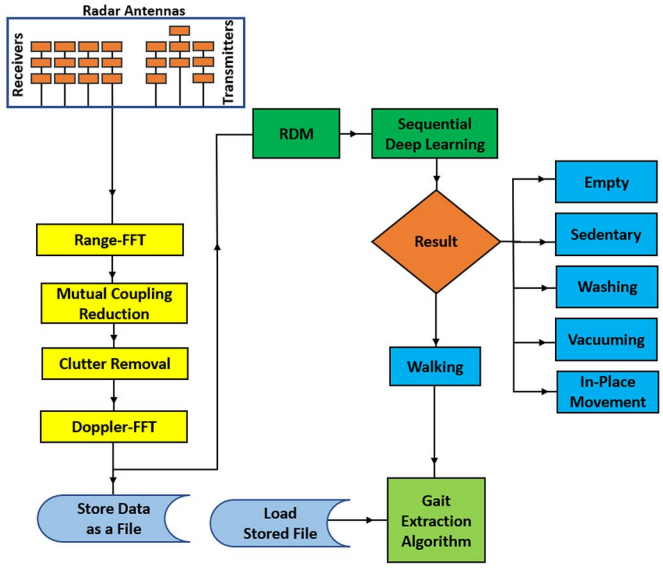

Fig. 3. AI-GM&AR System Flowchart. First, features for sequential deep learning will be provided and delivered to the network. If walking periods are identified, a gait extraction algorithm will be applied.

Algorithm 2 In-Home Activity Recognition Algorithm

check_status_of_livingroom (chirp):
Input: Radar Raw Data in Livingroom (Radar Unit #1)
Output: Type of Activity in the Living Room
chirp=capture_radar_raw_data_from_livingroom ()
fft=fast_fourier_transform (chirp)
complex=fft [0:int (fft.size/2)]
mcr=mutual_coupling_reduction(complex)
cr=clutter_removal (mcr)
R_P=save_in_database (cr)
RDM=fft (R_P)
result=GRU (RDM)
if result== "empty"
return "empty"
if result== "sedentary"
return "sedentary"
if result== "washing"
return "washing"
if result== "vacuuming"
return "vacuuming"
if result=="in_place_movement"
return "in_place_movement"
if result== "walking"
return gate_extraction (data)

range-FFT is applied to the received chirp samples from the FMCW radar to obtain the range information [51]. Mutual coupling reduction is applied to remove leakage from the transmitter antennas to the receiver antennas.

In received signals, there are two types of clutter effects: 1) stationary clutter and 2) time-varying clutter (ghosts) [26]. The direct reflection from stationary or unanimated objects is called stationary clutter. A stationary clutter removal algorithm is applied to the range profile to remove signals reflected from stationary clutter [26]. The average value of the signal is computed and subtracted from the aggregated signals; removing the average is equivalent to eliminating the stationary scatters. However, the interaction between a subject and stationary objects creates multipath or ghosting effects [26]. Multipath occurs when a signal takes two or more paths from the transmitting antenna to the receiving antenna. The number and particular behavior of the multiple paths depends on the room structure and the presence of moving subjects. The multipath issue is more significant when people move in the space occupied by reflective objects since moving even a small object in such an environment causes changes in multipath reflections [26]. Therefore, after performing the stationary clutter removal algorithm, the remaining signals in the range profile are direct signals from the subject, caused by chest motions (breathing) and other motions created by performing in-home activities, and multipath effects [26]. In this article, it will be demonstrated that deep learning can classify in-home activities despite the existence of multipath effects or ghosts. Since the human body is nonrigid, reflections from a human body occupy multiple cells of range bins in the range profile. Also, human locomotion, including walking, is a complex motion and the velocity of each segment of the human body performing different tasks varies over time [29], [34], [35], [36], [37], producing various micro-Doppler shifts in scattered signals. Applying the second FFT on a series of radar chirps (i.e., frame), an RDM is obtained. Therefore, using an FMCE radar, we simultaneously provide an RDM at each frame containing range and micro-Doppler signatures of a subject's in-home activities. As shown in [26], azimuth information is also needed to extract gait parameters that are out of this article's scope.

In this article, given that our target is a single subject, we use the entire RDM to train the model. This simplicity helps us avoid other signal processing such as detection (to capture occupied bins), clustering methods to cluster the detected bins, and then association algorithms to associate new bins to the previously occupied bins. We consider only one subject in this article because the main application of the AI-GM&AR system is in long-term care facilities or retirement homes, where only one subject is monitored.

Any in-home gait extraction method is prone to failure if the system is not intelligent enough to identify a human's in-home activities and differentiate between them. The system should provide precise and accurate gait data and be able to track a person's in-home activities over long periods. The system should be able to identify the type of in-home activities a subject performs. Six classes are defined in this article: 1) "Empty;" 2) "Sedentary;" 3) "Washing;" 4) "Vacuuming;" 5) "In-Place Movement;" and 6) "Walking." These are some of the activities a person performs during a typical day. Algorithm 2 shows the pseudo-code of the proposed activity recognition algorithm. As shown, the deep learning network would predict the type of activity a person is performing and send out the result as the current status. For the case of detected walking periods, a gait extraction algorithm [26] will be applied to the stored RDM samples to obtain gait values.

A. Deep Learning for the AI-GM&AR System

Due to the complexity of human motion, complex signal processing is required to map the RDM patterns to a human's specific activity, which is mathematically not feasible [53]. For this reason, we have chosen to adopt machine learning as an effective tool for our AI-GM&AR system. Our previous work [22] used a Random Forest classifier to identify walking periods from other in-place movements. However, conventional machine learning algorithms are limited in their capacity to fully capture the rich information contained in complex data, particularly time-varying samples [53]. Our proposed system in this article leverages deep learning approaches [54] to use the resulting time-varying signatures of the subject being monitored. Using multiple deep layers in a single network enables the efficient extraction of a subject's features and the building of a classification boundary [53].

Many deep learning models have shown exceptional promise in radar-based human activity recognition systems [28], [29], [30], [31], [32], [33]. The raw data is commonly converted into a 2-D spectrogram using the STFT method while being treated as an optical image. The corresponding architectures, such as 2-D convolutional neural networks (2D-CNNs), are used in these systems. However, since a human body motion consists of a series of associated postures through time, as will be shown in this article, ignorance of temporal characteristics leads to a complex network with a huge number of parameters but limited recognition accuracy. For this reason, CNNs are not a good algorithm for such time-varying data.

On the other hand, deep recurrent neural networks (DRNNs) have successfully addressed classification problems that feature temporal sequences [54]. DRNNs use a hidden node as memory, passing previous information to the next state for processing sequential inputs. Through this process, a DRNN can extract the temporal features of data. Long short-term memory (LSTM) and GRU are the two common models for sequential learning [53]. Due to the complex structure of a single LSTM unit, the LSTM network contains many parameters and so requires a larger sample size. LSTM contains three gates: 1) the forget gate; 2) the input gate; and 3) the output gate.

On the contrary, a GRU network has a simpler structure and fewer parameters. A GRU network includes only the reset gate and the update gate. From a spatial complexity perspective, LSTM has more parameters than GRU, therefore GRU has fewer computation costs than LSTM [47]. In this article, we show that the RDM has enough features for a single subject in-home monitoring, and the GRU network is a promising model to be used for time-varying RDMs of human activity classification. We demonstrate that GRU achieves sufficient recognition accuracy with relatively low complexity without the need for the subject's point cloud information [48]. The advantages of RDM, compared to point cloud information, are that such a system can provide valuable information using only one single transmitter and a receiver. Additionally, preprocessing is faster and simpler. An alternative approach using point cloud information would require an expensive high-resolution radar and complex signal processing.

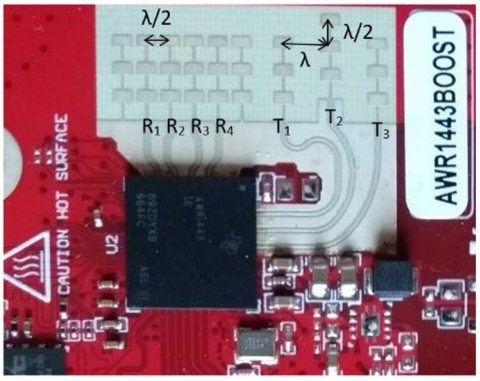

Fig. 4. AWR1443Boost PCB antenna.

V. Experimental Results

A. Our Devices

Our radar sensors are mm-wave FMCW radar systems (from TI Co. Ltd) [55]. Our system uses only one AWR1443Boost radar for each room. As shown in Fig. 4, the radar system has three transmitters (Tx_1, Tx_2, and Tx_3) and four receivers (Rx_1, Rx_2, Rx_3, and Rx_4), allowing the construction of an 8 and 4 virtual receiver array in azimuth and elevation, respectively. Note that we use the virtual receiver array to provide azimuth information of a subject to find the subject's position for extracting gait parameters [26]. We selected this MIMO radar in this article, although a single transmitter and receiver are enough for in-home activity recognition and walking period identification. This is because after detecting in-home random nonstraight-line walking periods, azimuth information of the subject is required in addition to the subject's range to get the subject's accurate position over time (velocity = position/time) [26]. We refer interested readers for more detail of obtaining azimuth information on a subject to our previous publications, where we used a Capon algorithm [41], [42].

To install the radar and find an appropriate location for the radar, we first analyzed the radar antenna radiation pattern. We simulated the radar antennas in a high-frequency structure simulator (HFSS) [56] and measured the radiation patterns. Interested readers can refer to our previous works [24], [25] that analyzed measured and simulated patterns of the radar antennas in detail. In this article, for simplicity, we just provided the simulated 3-D radiation patterns of the radar antenna in Fig. 5 to show the wide beam of the radar antennas. As Fig. 5(a) shows, the radar antennas provide a very wide beamwidth with more than 10-dBi gain. This wide beamwidth ensures wide coverage of the room. Fig. 5(b) shows the orientation of the radiation pattern and the antenna structure on the radar board, simulated in HFSS. Therefore, we chose to mount our devices on the wall that could cover the entire environment. The devices continuously emit and detect low-power wireless signals that reflect off nearby individuals. All signal processing pipelines are performed by a low-cost IoT Edge device without allocating an extra laptop or PC to run the signal processing.

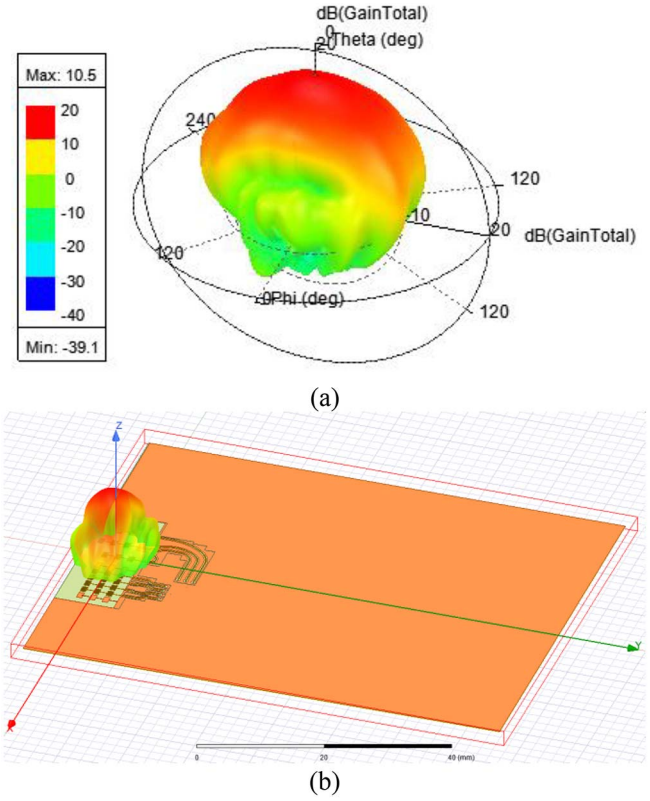

Fig. 5. HFSS simulation results of AWR1443Boost radar antenna (a) simulated 3-D radiation pattern (transmitting with Tx1) and (b) photograph of the simulated antenna structure along with its radiation pattern.

B. Radar Configuration

In this experiment, we use the following parameters for radar configuring: chirp duration: 380 μs, chirp slope: 43.03 MHz/μs, chirps per frame: 256, frame period: 98 ms, frequency bandwidth: 3602 MHz, operating frequency: 77 GHz, and A/D sampling rate: 4400 ksps. Using this configuration, the following parameters are obtained: maximum detachable range: 8.24 m, range resolution: 6.49 cm, velocity resolution: 0.02 m/s, and maximum velocity: 2.54 m/s.

C. Data Set Construction

As stated earlier, data sets collected by other researchers in this field were collected in controlled situations in a large environment with almost no clutter [20], [23], [28], [39], [43]. While this type of initial research is critical in developing practical systems, there needs to be research exploring how to computationally deal with subjects behaving naturally among everyday objects typically found in one's homes, as they would in a real home uncontrolled environment. Previous research reported in [21] explored a highly cluttered environment but in controlled scenarios using an expensive and complex high-resolution radar to create human point cloud information. However, no research has been reported on a single-sensor radar dealing with in-home gait and activity monitoring using RDMs. Since our goal is to provide an in-home activity recognition system, we collected data in a typical cluttered apartment. Fig. 6 depicts the living room area of the apartment where we conducted our experiment and collected our in-home data sets. This apartment is located in the research area of the Schlegel-University of Waterloo Research Institute for Aging (Schlegel-UW RIA). The living room has a typical highly cluttered environment with many reflective objects, similar to what would be found in a living room in any modern apartment building, including a TV, a fridge, metal window frames, and concrete floors and ceilings.

To compile this data set, we invited seven subjects to randomly walk in the apartment at their selected speed and perform various in-home activities without any predefined path to follow. If we walk or move in a highly cluttered environment, we create various multipath effects that should be removed from the actual signals from the subject [26], [57]. This effect adds more complexity to the signal processing chain in addition to the required high-resolution and complex radar sensors. To compile data sets in a typical home, we installed the radar sensor in a living room of an apartment, shown in Fig. 6. We defined six classes: 1) empty; 2) sedentary; 3) washing; 4) vacuuming; 5) in-place movement; and 6) walking. Our purpose for the "Empty" class was to identify the presence or absence of the subject in a living room. The result of the PAD algorithm and the deep learning will be combined to provide the final presence/absence status. The purpose of the sedentary class was to know how long the subject was sedentary (not active) during the day. This information could help the subject keep track of his/her daily activity and modify his/her future activities. Moreover, since most of the available vital signs detection algorithms are effective for a stationary subject, knowing whether a subject is stationary gives insight into the efficacy and confidence of breathing rate and heart rate algorithm outputs [58]. For instance, if it is determined that a subject is moving, it may be best to withhold these estimates until the subject is stationary to avoid giving erroneous results [58].

The washing, vacuuming, and in-place movement classes were defined in order to differentiate these activities from periods of walking and to track the subject's daily activities that involve movement other than walking. It is important to identify periods of walking, as defined by the walking class, to apply gait extraction algorithms accurately. Failure to properly identify walking periods can result in errors in gait data over time when applying gait extraction algorithms to non-walking activities. Any small error in gait parameters would cause misleading information in prediction and any subsequent proactive attempts (i.e., fall prevention) [11], [59], [60].

For data set construction, seven young and healthy subjects (three females and four males with heights ranging from 156 to 187 cm) performed their normal and natural daily life in the apartment. These are the protocols we followed for in-home data set construction.

1) For the empty class:
   a) no subject was in front of the radar, and no live body occupied the room.
2) For the sedentary class:
   a) a subject was sitting still at different places on sofas/chairs;
   b) a subject was sitting at various locations on sofas while working with a cell phone;

Fig. 6. In-home environment experiment conducted in Schlegel-UW RIA. The radar is used to collect data for the local system to train and validate deep learning networks.

c) a subject was sitting at various locations on sofas while working with a laptop;
d) a subject was sitting at various locations on sofas in the usual way (i.e., talking, moving his body, leg displacement, etc.);
e) a subject was sitting at various locations on sofas facing back and toward the radar.

3) For the washing class:
a) a subject was washing dishes in the kitchen;
b) a subject was drying the dishes;
c) a subject was putting the dried dishes into the cabinets;
d) a subject was cleaning the cabinets/ sink areas.

4) For the vacuuming class:
a) a subject was vacuuming the entire living room, even behind desks and coffee tables, in a typical way.

5) For the in-place movement class:
a) a subject was working out;
b) a subject was squatting;
c) a subject was picking objects from tables/floors;
d) a subject was sitting and standing from a chair.

6) For the walking class:
a) a subject was randomly walking in different directions in the entire living room, even behind desks and coffee tables, at his own selected speed.

In this study, data sets were collected with subjects moving naturally without being asked to move to a specific location. Therefore, it can be concluded that the data is not dependent on the radar's relative position. However, it is possible that the washing class may be dependent on the radar position due to the static nature of the activity in close proximity to the sink. A total of 310357 RDMs were generated from data collected from seven participants, who each completed five different in-home activities for a total of 50 min of data. Each participant completed each task for approximately 10 min, resulting in approximately 7400 frames of data per class per subject. The labeling of the data is based on the order in which the tasks were completed, with some potential for minor labeling errors due to the subjects not perfectly following the requested activity for the full 10 min. These errors may include deviations from the requested activity, such as temporary pauses or walking while holding equipment. While efforts were made to minimize these errors, they were hard to control. For example, participants might have stopped vacuuming intermittently or walked while holding the vacuum instead of consistently vacuuming the floor. These flaws were simply very difficult to control.

D. Results

In this section, we provide samples of RDMs and STFT patterns of in-home activities. We then provide and compare the results of various deep learning networks fed by RDMs and STFT.

1) Range-Doppler Maps: An example of the RDM of each in-home activity is provided in Fig. 7. Each RDM is a matrix of 128 rows and 256 columns, normalized to its maximum. All RDMs shown here are the result of frame #100. Note that frame #100 in Fig. 7 is just an example of each activity in this article, while other frames also show the details of each activity. The horizontal and vertical axes represent the subject's range (radial distance) and velocity, respectively. The RDM in Fig. 7(a) is for the empty room (when no subject was in the room). As shown in Fig. 6, although there are several objects in the living room, the RDM of the empty room shows some random noise after performing the clutter removal algorithm. Fig. 7(b) is the RDM of the environment when a subject was sitting on the sofa. The velocity shown is around -0.02 to 0.02 m/s (mainly from the chest motion), with the occupied range bins from $R = 3.11$ m to $R = 3.24$ m. Comparing Fig. 7(a) and (b), the effectiveness of our stationary clutter removal algorithms are shown. It is demonstrated that subtracting the average signal value from the integrated signals eliminates the direct effects of the stationary objects (i.e., stationary clutter).

Fig. 7(c) shows the RDM when the subject was standing by the sink washing dishes at an approximate $R = 6.5$ m.

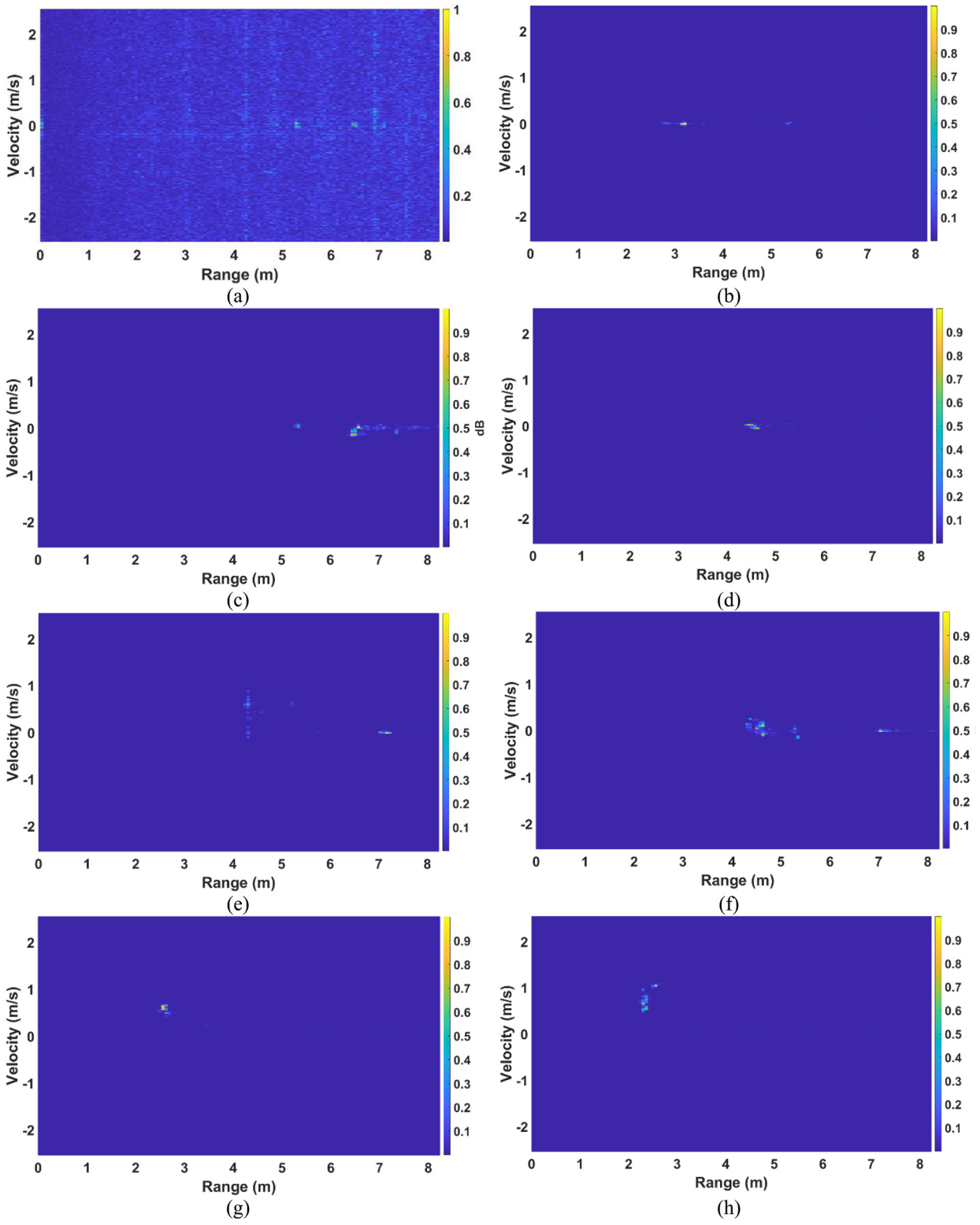

Fig. 7. RDMs of (a) an empty room (frame #100), (b) a subject sitting on a sofa (frame #100), (c) a subject washing dishes (frame #100), (d) a subject picking up an object (frame #100), (e) a subject vacuuming (frame #100) (f) a subject vacuuming (frame 105) (g) a subject walking (frame #100) (h) a subject walking (frame #105).

As shown, since the subject was at a close distance from a metallic object (the fridge in the kitchen), the interaction of the reflected signals from his body and the fridge created multipath effects (ghosts or time-varying clutter) [26], [57] observed at $R = 6.5$ m extended to $R = 8$ m. The multipath effect is more significant when the subject moves, particularly near reflective materials such as metal [26], [57]. Ghosts are visible for the case of vacuuming in Fig. 7(e) and (h) when

the subject was at an approximate range of $R = 4.5$ m away from the radar, while ghosts are visible at $R = 7$ m and further. Interested readers can refer to our previous works that detailed multipath effects in a cluttered environment published in [26]. One of the drawbacks of using point cloud information [21] to train machine learning is that ghosts' signals will be detected as a point cloud. Therefore, an even more sophisticated technique is needed to deal with ghosts and distinguish ghosts from the subject's direct reflections to be fed to machine learning. However, since the entire RDM is fed to our deep learning model without any handcrafted feature extraction method, the deep learning model handles ghost signals and predicts the classes based on what has been trained. The RDM of the environment with a subject picking up an object from the floor is provided in Fig. 7(d). The subject's body created velocity (micro-Doppler in radar received signals) ranging from -0.08 to 0.02 m/s while range bins were occupied from $R = 4.34$ m to $R = 4.67$ m. For the case of vacuuming and walking [Fig. 7(e)–(h)], since the subject had movement and the RDMs changed significantly frame by frame, we provided the RDMs at two different frames (#100 and #105) to provide more details. The subjects occupied multiple velocities and range bins for these two activities. For each of these activities, the RDMs are slightly different, so the deep learning model can extract sufficient features to distinguish them and identify the type of activity a subject is performing.

2) Deep Learning Results: To train and test machine learning algorithms, we followed two different validation approaches: 1) a K-fold validation method and 2) a new person. For the first one, we used a 5-fold validation method, 80% of the whole data is used for training, and 20% for testing [21]. Moreover, to assess our deep learning network, it is essential to have a completely unseen subject for the test set to validate the network architecture and ensure the generality of the network in a real-life application. Although with the K-fold validation method, the samples are unseen in testing, the subjects are seen. With the second method, we intend to generalize our trained model to be functioning for any new person. With the K-fold method, the activity patterns of all subjects are seen, while with the second method, the activity patterns of a new person are unseen for the network.

To show the robustness and effectiveness of our proposed method for human activity recognition and gait period identification, we provided the outcomes of three procedures.

1) Train set based on RDM samples collected from six subjects performing various in-home activities at the apartment (living room), and the test set on samples collected from the seventh subject (Scenario #1).
2) The K-fold method using RDM samples collected from all seven subjects performing various activities at the apartment (Scenario #2).
3) Train set based on STFT patterns collected from six subjects performing various in-home activities at the apartment (living room), and the test set on samples collected from the seventh subject (Scenario #3).

Since the performance of deep learning networks highly depends on their hyper-parameters to control how it learns the training data set, optimizing the hyper-parameters utilized by each network is necessary. To find the best hyper-parameters for deep learning networks, a range of values was specified for five crucial hyper-parameters: 1) learning rate; 2) batch size; 3) activation function; 4) optimization algorithm; and 5) the number of layers. Several deep learning models were implemented to find the best model for our in-home activity recognition system. For all local processing in this article (to train deep learning models), we used a computer system with Windows 10 64 bits operating system and an Intel Xeon CPU E5-1603 v4 @ 2.4-GHz 128-GB RAM processor. We implemented deep learning networks in TensorFlow (Keras) with a cross-entropy loss function in 50 epochs. Our criteria for choosing the best model were the performance in terms of accuracy and execution prediction time. The motivation to use accuracy as the performance metric in this work is that we have balanced data sets, so the models are not biased. Confusion matrices of four different deep learning models fed by RDMs, including 2D-CNN, 2D-CNNLSTM, LSTM, and GRU are provided in Fig. 8 for scenario #1. A summary of the performance of all four models is listed in Table I.

TABLE I
COMPARISON OF THE RESULT OF DIFFERENT DEEP LEARNING MODELS (TEST DATA: A NEW PARTICIPANT)

Model	Inputs	Accuracy	Testing Time/Sample
GRU	STFT	75%	2.4 *ms*
LSTM	STFT	67%	6.9 *ms*
2-DCNN	STFT	69%	10.7 *ms*
1-DCNNLSTM	STFT	73%	4.7 *ms*
2-DCNN	RDM	84%	3.5 *ms*
GRU	RDM	86%	0.3 *ms*
LSTM	RDM	87%	1.2 *ms*
2-DCNNLSTM	RDM	85%	3.7 *ms*

LSTM is the most accurate network in identifying the six in-home classes, while 2-DCNN is the least precise model. The total accuracy of 2-DCNN, 2-DCNNLSTM, LSTM, and GRU models is 84%, 85%, 87%, and 86%, respectively. All models identify the empty room 100% accurately, meaning that an occupied/ vacant room will be recognized without any error.

2-DCNNLSTM and LSTM models classify the sedentary, in-place movement, and washing classes with less than 6% error. 2-DCNNLSTM, GRU and LSTM models can recognize walking periods and distinguish them from other activities with more than 70% accuracy. However, the CNN model performs poorly in identifying the walking periods. As seen, all recurrent neural networks performed better in predicting in-home activities, particularly walking. This is because these networks exhibit temporal dynamic human behavior, whereas CNN mainly extracts spatial features without considering the timing effect of in-home activity patterns. The most challenging class for all four networks is vacuuming which is confused with walking and in-place movement. The reason for this poor performance will be further analyzed in this article. In addition to the accuracy, as shown in Table I, the execution prediction time of CNN and 2-DCNNLSTM is much longer

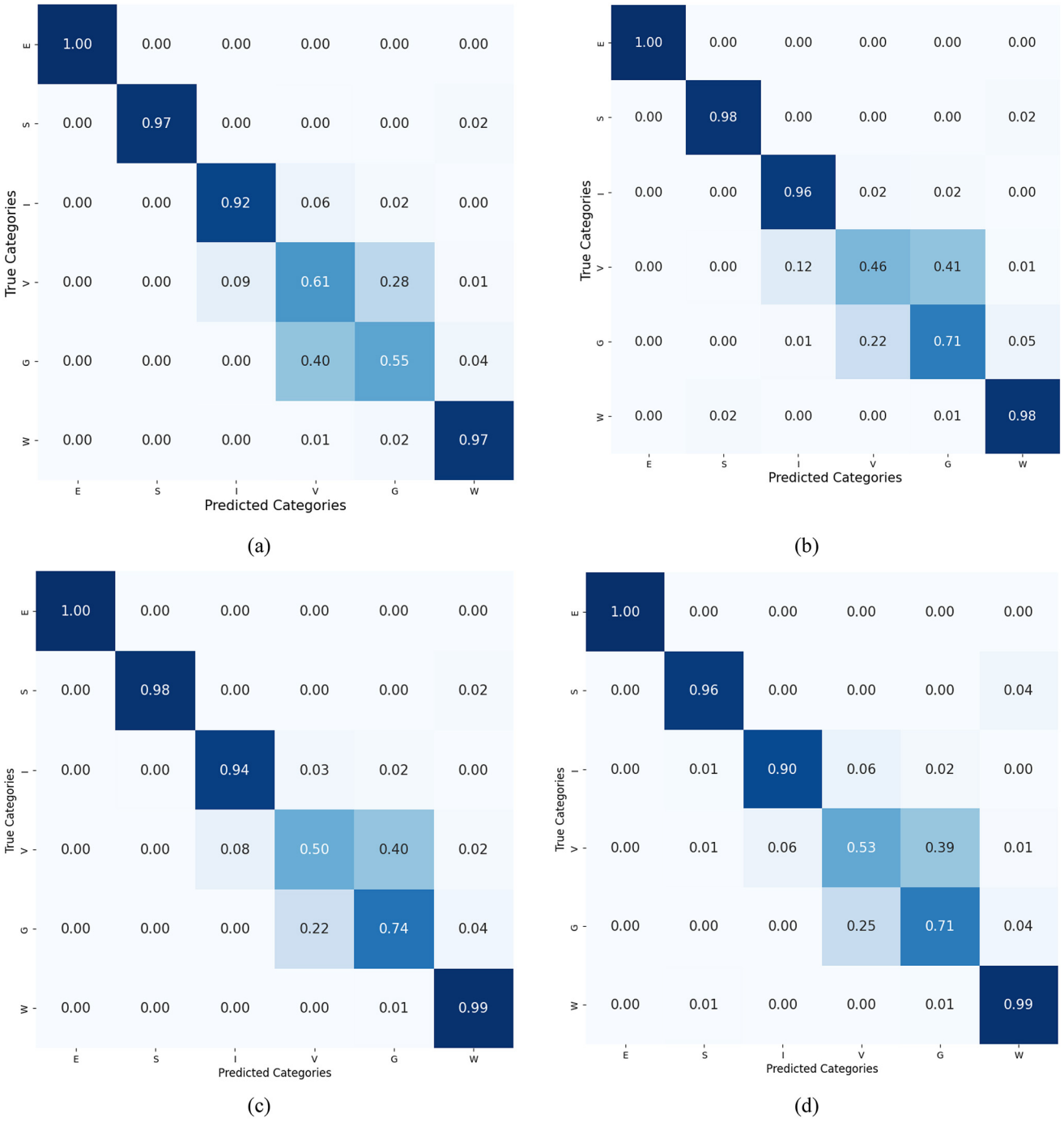

Fig. 8. Confusion matrix yielded by the different networks, fed by RDMs, applied to test data sets (data collected from a complete new subject, Scenario #1) in a living room environment: (a) 2-DCNN, (b) 2-DCNNLSTM, (c) LSTM, and (d) GRU. Note that "E," "S," "I," "V," "G," and "W" stand for empty, sedentary, in-place movement, vacuuming, walking, and washing, respectively.

than the other networks because of the complexity of the convolution-based neural networks. LSTM and GRU networks are more accurate and faster for in-home activity recognition. We deploy the GRU network for our real-time processing since it is faster in predicting a new class which is almost as accurate as the LSTM network in predicting the in-home activities of a new subject. Graphs of the performance of the accuracy and the loss function of the GRU network are plotted in Fig. 9.

The GRU network performance in predicting in-home activities of an unseen subject (Scenario #1) ensures the generality.

However, it is common to train a model based on a known subject to classify and monitor his future activities. Therefore, for Scenario #2, we analyze the GRU network in predicting new activities while the patterns of subject's activities were previously trained. It should be pointed out that other networks were assessed for Scenario #2. We provide the outcome of GRU as it yields the best performance. The confusion

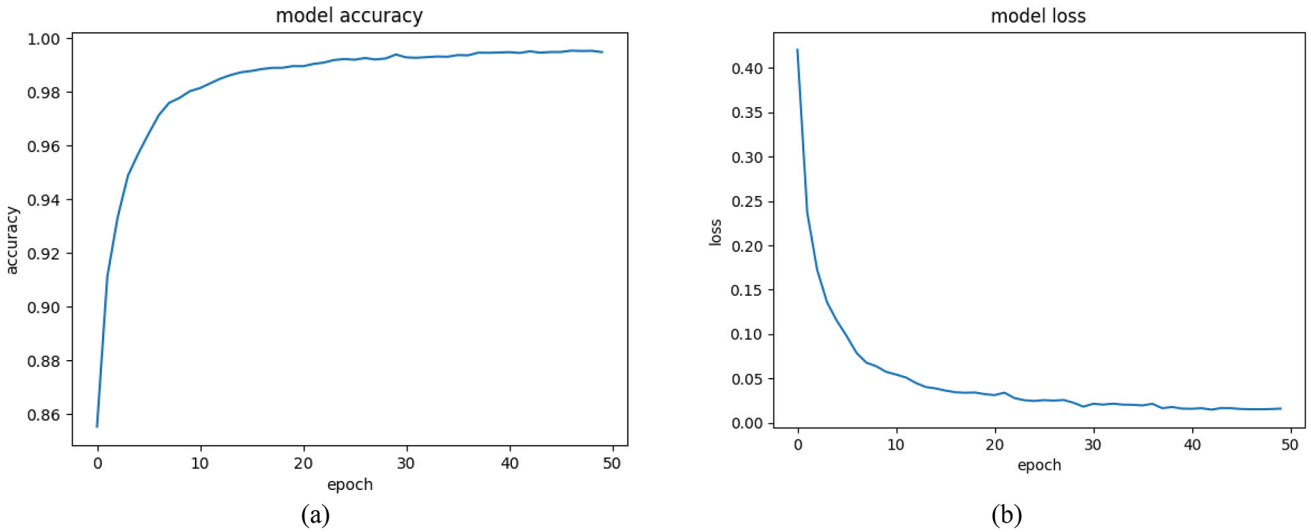

Fig. 9. Graphs of the performance of (a) accuracy and (b) loss function of the GRU network in each epoch.

matrix of the GRU network for Scenario #2 is provided in Fig. 10. The overall accuracy of this case is 93%. The network performance improved significantly because the network was trained based on all subjects' activity patterns. In this case, the GRU model predicts sedentary, washing, and in-place movement with more than 97% accuracy. The model can identify walking periods with 87% accuracy, while vacuuming is still the least accurate class (75%). As seen in Figs. 8 and 10, some of the RDMs of vacuuming were misclassified in the walking class, leading to less accuracy in the vacuuming class.

Although the model was tuned and various variables were assessed, the reason for this lower accuracy should be analyzed. Since the model was carefully analyzed and tuned, we referred to the data sets. We found that some participants did not follow our order for vacuuming perfectly. Instead of cleaning the floor, some of our participants were walking while holding the vacuum cleaner. This sanity check was done based on the result of all RDMs over the entire data and STFT patterns. Participants also confirmed this. Since our labeling method was to ask each participant to do each task for 10 min consistently and we were not allowed to have a video recording, we stuck with this labeling method even though we found this flow in a small portion of our samples. To show the details of this flow, we provided the STFT patterns of two subjects in Fig. 11. Although nonstraight-line STFT patterns might not be easily distinguishable, we provided the STFT results because it clearly shows the variation over time in one plot. RDMs are much clearer and more informative, but a series of frames that take up a huge space in this article should be shown. As shown, since subject "A" followed what he was asked to do perfectly, the STFT pattern of him vacuuming [Fig. 11(a)] is completely different from his walking pattern [Fig. 11(b)]. However, subject "B" was not following our request and was not performing the actual vacuuming, and she was holding the vacuum cleaner while walking. The STFT pattern of her vacuuming [Fig. 11(c)] is very close to walking [Fig. 11(d)]. Therefore, we can conclude that the low accuracy of the vacuuming class is because of the data sets, not

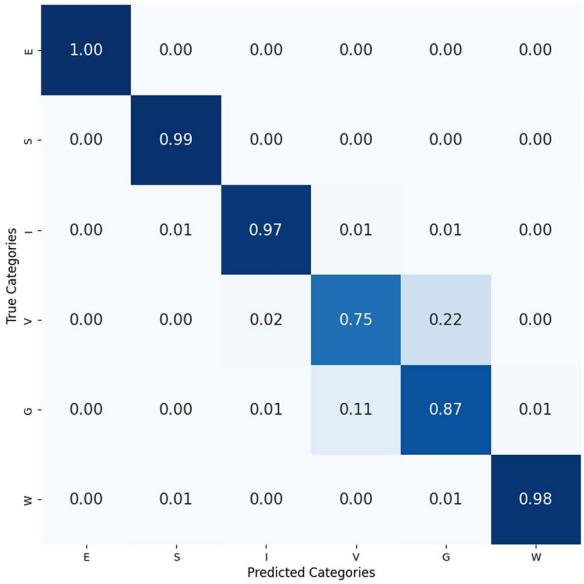

Fig. 10. Confusion matrix yielded by the GRU network, fed by RDMs, applied to test data sets (Scenario #2) in a living room environment.

the model. The model identifies some as walking because the participants walked instead of vacuuming.

Since many studies used STFT patterns as inputs for machine learning and deep learning models, we also train our deep learning models with STFT patterns. The purpose is to compare the results of deep learning networks fed by RDMs with the case of STFT inputs. To generate the STFT signature of each activity, we choose a small Hamming window for time-frequency analysis of the real-time radar human activities/gait signals. The length of the Hamming window is 128 samples.

As shown in Fig. 11, STFT patterns show the time-varying velocity created by each subject without considering the occupied range bins. Fig. 12 shows the network STFT inputs in detail. After optimizing the network parameters, the input is a vector of 1×256 consisting 25 ms of a subject's

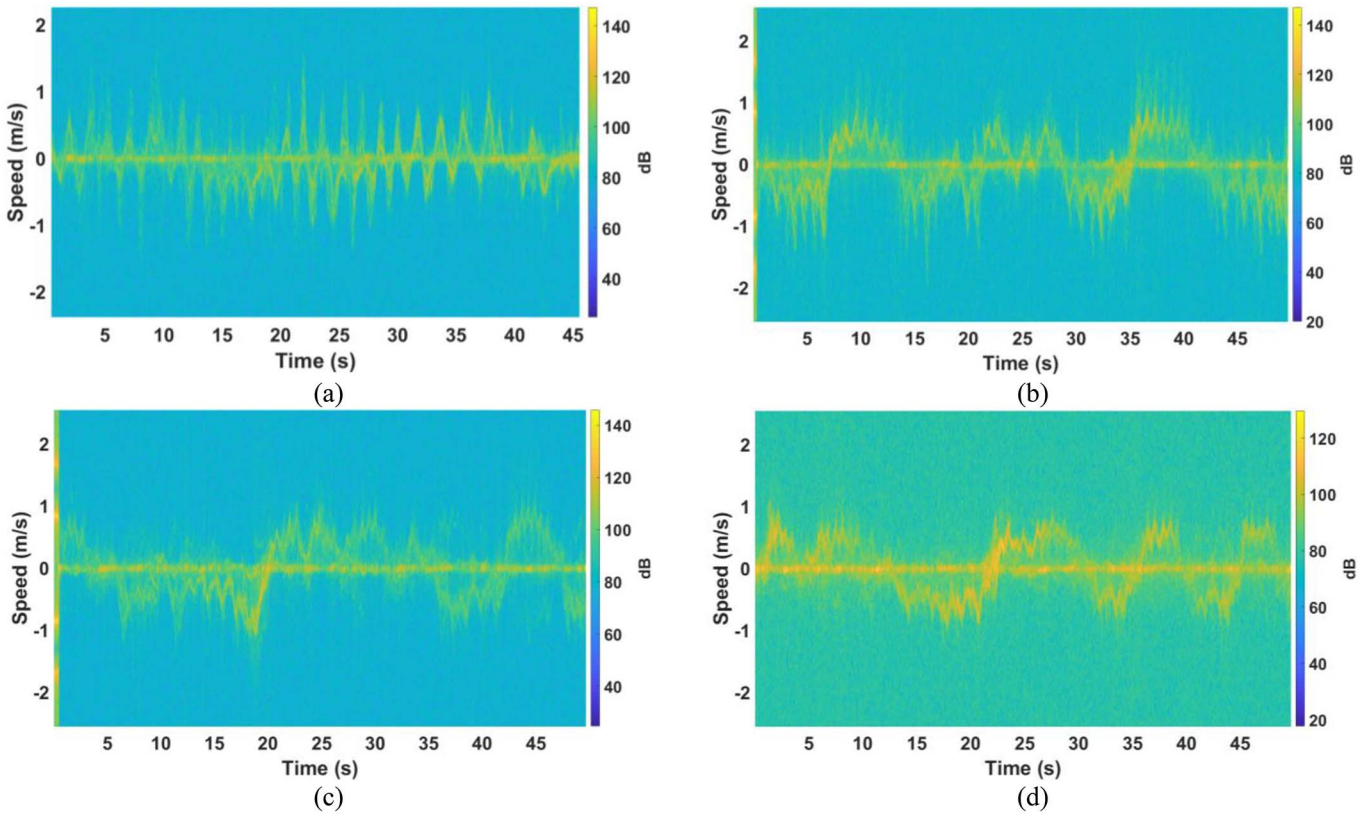

Fig. 11. STFT patterns of (a) subject "A" vacuuming, (b) subject "A" walking, (c) subject "B" vacuuming, and (d) subject "B" walking.

micro-Doppler signature. The total number of time steps is set to 50. Note that for the time steps, we observed that when it is greater or less than 50, the performance of the networks degrades. Therefore, the dimension of the input of the networks is (1, 50, 256). In total, $t = 25 \times 50 = 1250$ ms of the subject's spectrogram is fed to networks. Table I shows the summarized output of four networks fed by STFT patterns of Scenario #3.

As shown, GRU is the most accurate network in classifying activity patterns of a new subject. Comparing the performance of all four networks fed by RDMs, the network fed by STFT is less accurate. To detail the results, Fig. 13 shows the confusion matrix yielded by the GRU network fed by STFT patterns.

As seen, occupied versus empty rooms could be identified with 100% accuracy in this case as well. However, other classes are not predicted as accurately as the networks fed by the RDMs. For example, considering the RDMs as inputs for GRU, the sedentary class was identified 96% accurately, while it is 83% accurate in this case. The pattern of washing is also much less accurate in this case.

This is because the network has not received enough information to distinguish several classes. To show the detail, Fig. 14(a) and (b) show the STFT pattern of sitting on the sofa while working with a cell phone and washing dishes in the kitchen, respectively. The two patterns are not as distinguishable as the RDMs are in Fig. 7(b) and (c).

3) Output of the Proposed AI-GM&AR System: As mentioned, the GRU network is trained and optimized in a local machine. The tuned and optimized model with the parameters

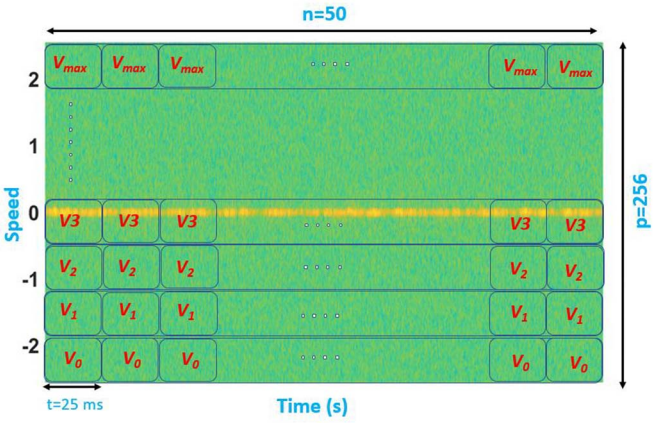

Fig. 12. STFT patterns as inputs for deep learning networks.

listed in Table II is then deployed into the cloud to be used in the run-time section. The network consists of multiple hidden layers, including the inputs, GRU cell layers, fully connected layers that combine all the features learned by GRU layers for classification, and the output layer. Therefore, the output size is equal to the number of classes. The SoftMax layer normalizes the output of the former layer to be used as classification probabilities.

Preprocessing is performed in the Raspberry Pi to prepare inputs for the PAD algorithm and the GRU network. Then, the real-time preprocessed data is sent to the Azure IoT Hub using Azure IoT Edge Runtime modules [49]. In Azure, data is collected and stored in the Azure SQL Database [50].

TABLE II
GRU NETWORKS HYPER-PARAMETERS

Hyper-parameters	Optimized values
Activation function	Rectified Linear Unit
Batch size	512
Number of layers	5
Learning rate	0.01
Optimization algorithm	Adam
Number of units for each layer	(256, 128, 64, 64, 6)

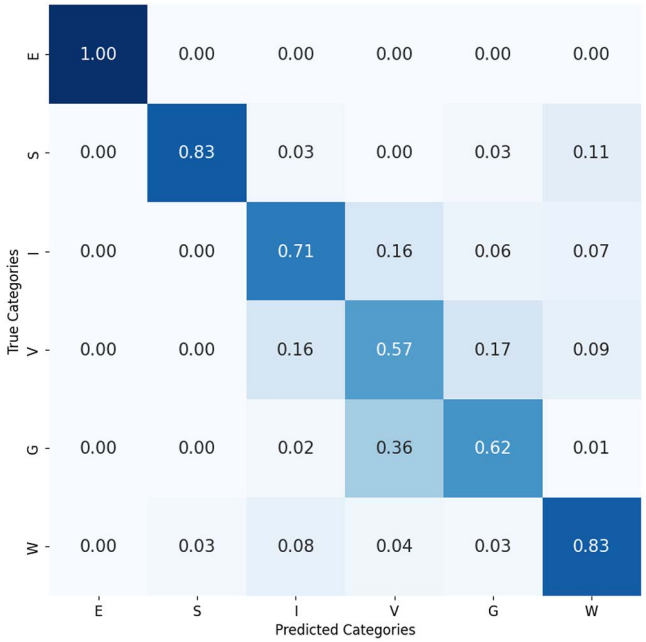

Fig. 13. Confusion matrix yielded by the GRU network, fed by STFT patterns, applied to test data sets (Scenario #3) in a living room environment.

Ultimately, the status of the subject in each room is kept in storage for the real-time BI (Business Intelligence) dashboard, as shown in Fig. 15. As shown, the BI dashboard consists of four sections: 1) a daily activity report depicted as a bar chart; 2) a gait speed report shown as a line chart; 3) current status illustrated as a predefined icon; and 4) extracted gait parameters. Therefore, the proposed cloud-based system provides a report of the subject's daily activity, tracks the current status, and captures and records gait parameters over time. Note that the gait extraction algorithms are beyond the scope of this article.

VI. DISCUSSION

Our findings suggest that continuous passive monitoring of activity within a home is feasible and has the potential to improve clinical practice for all individuals, not just older adults. The proposed monitoring system operates in the background, analyzing reflections of radio signals to record activity levels, daily variations, and changes over time without requiring intervention from the person being monitored. This information can be remotely transmitted to a healthcare provider in a timely manner, enabling safe and frequent health monitoring without requiring the subject to leave their home

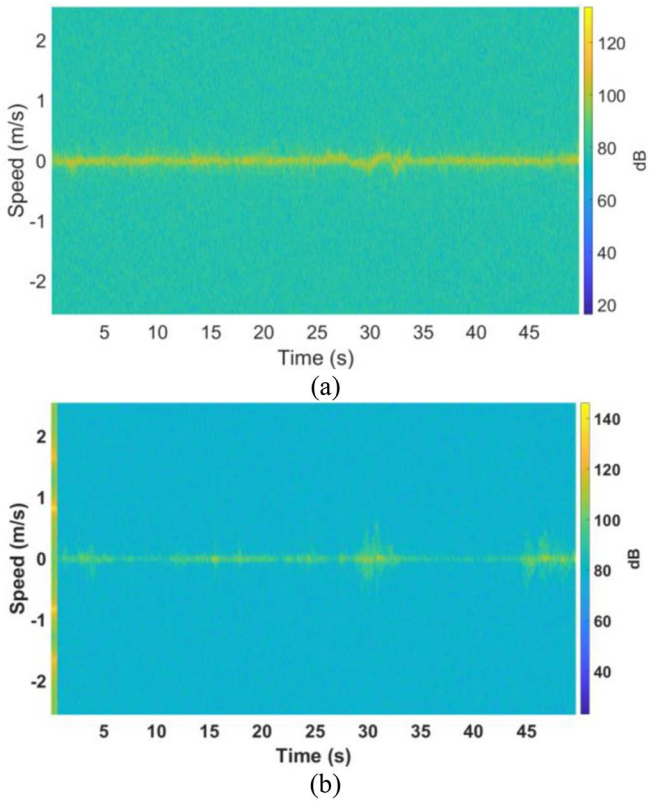

Fig. 14. Time series inputs: STFT patterns of a subject (a) sitting on the sofa and (b) washing dishes.

or actively self-report their measurements. This has significant implications, particularly in the context of COVID-19 social distancing measures and the increasing population of older adults and individuals with chronic illnesses. The findings of this study suggest that the in-home natural characteristics captured by the technology may have broader applications, including the potential to assess behavioral symptoms and predict the risk of hospitalization. This technology may also have clinical utility for the assessment of individuals with Parkinson's Disease, who may be underserved due to factors, such as living in rural areas or having limited mobility or cognitive impairment that make it difficult to leave home [15].

In this article, we used FMCW radars to provide RDMs. We considered RDMs as inputs for deep learning networks that resulted in more accurate outcomes compared with STFT inputs. This is because RDMs consist of time-varying information of both range and micro-Doppler, while STFT patterns only represent micro-Doppler features. Although the radar used in this study provides azimuth of the subject, we did not include azimuth information as inputs for deep learning models. There were three reasons behind this: 1) the RDM method is fast and easy-to-implement that a Raspberry Pi can handle and generate. However, to calculate azimuth, a eam-forming algorithm [41], [42] is a time-consuming process that is not fast enough for real-time application; 2) adding more features would lead to more complex models; the execution prediction time of a complex model is longer than a simpler model; and 3) RDMs provide enough features for our models to accurately predict new classes without needing more

Fig. 15. Prototype of the output of our BI dashboard of the proposed AI-GM&AR system. The BI dashboard consists of four sections: a daily activity report, a gait speed, the current status of the subject, and extracted gait parameters.

information. For real-time applications, we should consider simplicity and speed of processing as decisive and key factors. We used the MIMO system because the azimuth information of a subject is needed to calculate speed of nonstraight-line walking periods (velocity = position/time). Analyzing different deep learning models, we found the GRU networks faster while obtaining a similar accuracy as other more complex networks. Because of the complex structure of the LSTM and CNNLSTM networks, they contain many parameters and are slower comparatively.

In the more complex and comprehensive scenarios, the system demonstrated a slight decrease in accuracy when applied to new subjects but only misidentified a small number of nonwalking samples as walking. Despite the dependence of micro-Doppler patterns on the relative angle between the radar sensor and the subject, the GRU network was able to overcome this issue. We demonstrated that when the network is trained on a range of RDMs representing various activities, it is able to accurately predict new scenarios, regardless of the direction of walking or the type of activity being performed. As such, the proposed system could handle new subjects without any restrictions.

There are several limitations to this study. First, the participants were only monitored within our living-space research apartment and within the range of the radio devices. Second, the evaluation of the system is limited by the accuracy of the subjects' adherence to the requested tasks and the self-reported labels. The labeling process can be challenging when camera recordings are not allowed. The labels for each class may be affected by the subjects' activities at each frame, resulting in potential flaws in the data sets. Third, this study was designed for a single subject, and future research will be needed to accommodate multiple residents within a single home. Fourth, various causes for gait impairments were not studied in this article [49]. Some impairments, such as falls and gait freezing, can be captured by our system and provide a natural topic for future work. Despite the aforementioned limitations, we believe that the study provides important insights and addresses key unmet needs in independent living.

VII. Conclusion

In this work, we present a cloud-based in-home activity recognition and walking period identification system that utilizes IoT-based millimeter-wave FMCW radar sensors and sequential deep learning to generate data streams of naturally occurring human activities within the home environment. By leveraging the abundance of continuous data, the proposed system is capable of accurately identifying the type of activity being performed by a subject. This system represents a significant advancement in the development of autonomous continuous human monitoring systems as it not only detects walking periods and recognizes the type of activity but also has the potential to report on the activity level of the subject (e.g., sedentary versus active) and various other parameters, such as washroom usage frequency and sleep duration.

To evaluate the performance of the proposed system, we compiled a data set of millimeter-wave data collected from subjects performing various activities within their own homes, representing a unique and first-of-its-kind resource for this purpose. In contrast to existing data sets for human activity recognition and gait analysis that have been collected

in constrained, artificially controlled environments and have focused on simple yet-realistic activities and straight-line walking periods, our data set captures naturally occurring human activities in a familiar and commonly used living-space environment. Utilizing RDMs of a single subject performing various activities in their living environment as input, we trained a deep GRU network to classify in-home activities in the cloud. We performed two methods of network evaluation: 1) a K-fold validation, where the network assessment was done with newly collected samples, but the subjects were previously seen and 2) an assessment based on a new subject. Our results demonstrate that the deep GRU network is able to achieve an accuracy of 93% for known subjects and 87% for a new subject performing select in-home activities. In future work, we plan to further investigate the capabilities of millimetre-wave-based human activity recognition and gait monitoring in more dynamic scenarios.

ACKNOWLEDGMENT

The authors would like to thank all participants who participated in this study. The authors also thank Christopher Lehman for the stimulating discussions and for proofreading this manuscript. This study was conducted in the living-space research apartment at the Schlegel-University of Waterloo Research Institute for Aging.

REFERENCES

[1] S. Chen, J. Lach, B. Lo, and G. Z. Yang, "Toward pervasive gait analysis with wearable sensors: A systematic review," *IEEE J. Biomed. Health Inform.*, vol. 20, no. 6, pp. 1521–1537, Nov. 2016, doi: 10.1109/Jbhi.2016.2608720.

[2] N. M. Peel, S. S. Kuys, and K. Klein, "Gait speed as a measure in geriatric assessment in clinical settings: A systematic review," *J. Gerontol. A Biol. Sci. Med. Sci.*, vol. 68, no. 1, pp. 39–46, 2013, doi: 10.1093/Gerona/Gls174.

[3] A. Middleton, S. L. Fritz, and M. Lusardi, "Walking speed: The functional vital sign," *J. Aging Phys. Activity*, vol. 23, no. 2, pp. 314–322, 2015, doi: 10.1123/Japa.2013-0236.

[4] D. Jarchi, J. Pope, T. K. M. Lee, L. Tamjidi, A. Mirzaei, and S. Sanei, "A review on accelerometry-based gait analysis and emerging clinical applications," *IEEE Rev. Biomed. Eng.*, vol. 11, pp. 177–194, Feb. 2018, doi: 10.1109/Rbme.2018.2807182.

[5] J. Perry and J. M. Burnfield, "Gait analysis: Normal and pathological function," *J. Sports Sci. Med.*, vol. 9, no. 2, p. 353, 2010.

[6] A. K. Welmer, D. Rizzuto, C. Qiu, B. Caracciolo, and E. J. Laukka, "Walking speed, processing speed, and dementia: A population-based longitudinal study," *J. Gerontol. A, Biol. Sci. Med. Sci.*, vol. 69, no. 12, pp. 1503–1510, 2014, doi: 10.1093/Gerona/Glu047.

[7] G. A. Van Kan et al., "Gait speed, body composition, and dementia. The EPIDOS-Toulouse cohort," *J. Gerontol. A, Biol. Sci. Med. Sci.*, vol. 67, no. 4, pp. 425–432, 2012, doi: 10.1093/Gerona/Glr177.

[8] R. Schniepp et al., "Increased gait variability is associated with the history of falls in patients with cerebellar ataxia," *J. Neurol.*, vol. 261, no. 1, pp. 213–223, 2014, doi: 10.1007/S00415-013-7189-3.

[9] M. L. Callisaya et al., "Gait, gait variability and the risk of multiple incident falls on older people: A population-based study," *Age Ageing*, vol. 40, no. 4, pp. 481–487, 2011, doi: 10.1093/Ageing/Afr055.

[10] C. Y. Hsu, Y. Liu, Z. Kabelac, R. Hristov, D. Katabi, and C. Liu, "Extracting gait velocity and stride length from surrounding radio signals," in *Proc. Conf. Human Factors Comput. Syst.*, May 2017, pp. 2116–2126, doi: 10.1145/3025453.3025937.

[11] K. E. Webster, J. E. Wittwer, and J. A. Feller, "Validity of the GaitRite walkway system for the measurement of averaged and individual step parameters of gait," *Gait Posture*, vol. 22, no. 4, pp. 317–321, 2005, doi: 10.1016/J.Gaitpost.2004.10.005.

[12] A. Pfister, A. M. West, S. Bronner, and J. A. Noah, "Comparative abilities of Microsoft Kinect and Vicon 3D motion capture for gait analysis," *J. Med. Eng. Technol.*, vol. 38, no. 5, pp. 274–280, 2014, doi: 10.3109/03091902.2014.909540.

[13] W. Tao, T. Liu, R. Zheng, and H. Feng, "Gait analysis using wearable sensors," *Sensors*, vol. 12, no. 2, pp. 2255–2283, 2012, doi: 10.3390/S120202255.

[14] A. Muro-De-La-Herran, B. García-Zapirain, and A. Méndez-Zorrilla, "Gait analysis methods: An overview of wearable and non-wearable systems, highlighting clinical applications," *Sensors*, vol. 14, no. 2, pp. 3362–3394, 2014, doi: 10.3390/S140203362.

[15] Y. Liu et al., "Monitoring gait at home with radio waves in Parkinson's disease: A marker of severity, progression, and medication response," *Sci. Transl. Med.*, vol. 14, no. 663, Sep. 2022, Art. no. eadc9669, doi: 10.1126/scitranslmed.adc9669

[16] S. Z. Gurbuz, C. Clemente, A. Balleri, and J. J. Soraghan, "Micro-Doppler-based in-home aided and unaided walking recognition with multiple radar and sonar systems," *IET Radar, Sonar Navig.*, vol. 11, no. 1, pp. 107–115, 2017, doi: 10.1049/Iet-Rsn.2016.0055.

[17] X. Ma, R. Zhao, X. Liu, H. Kuang, and M. A. A. Al-Qaness, "Classification of human motions using micro-Doppler radar in the environments with micro-motion interference," *Sensors*, vol. 19, no. 11, p. 2598, 2019, doi: 10.3390/S19112598.

[18] D. Tahmoush and J. Silvious, "Gait variations in human micro-Doppler," *Int. J. Electron. Telecommun.*, vol. 57, no. 1, pp. 23–28, 2011, doi: 10.2478/V10177-011-0003-1.

[19] A. K. Seifert, M. G. Amin, and A. M. Zoubir, "Toward unobtrusive in-home gait analysis based on radar micro-Doppler signatures," *IEEE Tran. Biomed. Eng.*, vol. 66, no. 9, pp. 2629–2640, Sep. 2019, doi: 10.1109/Tbme.2019.2893528.

[20] K. Saho, K. Uemura, K. Sugano, and M. Matsumoto, "Using micro-Doppler radar to measure gait features associated with cognitive functions in elderly adults," *IEEE Access*, vol. 7, pp. 24122–24131, 2019, doi: 10.1109/ACCESS.2019.2900303.

[21] Y. Kim, I. Alnujaim, and D. Oh, "Human activity classification based on point clouds measured by millimeter wave MIMO radar with deep recurrent neural networks," *IEEE Sensors J.*, vol. 21, no. 12, pp. 13522–13529, Jun. 2021, doi: 10.1109/Jsen.2021.3068388.

[22] H. Abedi, C. Magnier, J. Boger, and A. Wong, "Integration of random forests and MM-wave FMCW radar technology for gait recognition," *J. Comput. Vis. Imag. Syst.*, vol. 5, no. 1, p. 2, 2019.

[23] H H. Abedi, G. Shaker, J. Boger, P. Morita, and A. Wong, "Use of millimeter wave FMCW radar to capture gait parameters," *Amer. J. Biomed. Sci. Res.*, vol. 2, pp. 122–123, Nov. 2019, doi: 10.34297/Ajbsr.2019.06.001009.

[24] H. Abedi, P. P. Morita, J. Boger, A. Wong, and G. Shaker, "In-package integrated dielectric lens paired with a MIMO mm-Wave radar for corridor gait monitoring," in *Proc. IEEE Int. Symp. Antennas Propag. USNC-URSI Radio Sci. Meeting (APS/URSI)*, Feb. 2022, pp. 1795–1796, doi: 10.1109/APS/URSI47566.2021.9704192.

[25] H. Abedi et al., "In-package integrated 3D-printed dielectric lens for a milimiter-wave radar," *IEEE Trans. Compon. Packag. Manuf. Technol.*, unpublished.

[26] H. Abedi, J. Boger, P. P. Morita, A. Wong, and G. Shaker, "Hallway gait monitoring using novel radar signal processing and unsupervised learning," *IEEE Sensor J.*, vol. 22, no. 15, pp. 15133–15145, Aug. 2022, doi: 10.1109/JSEN.2022.3184188.

[27] "Google's new smart display tracks your sleep using radar—Google assistant." The Guardian. 2021. [Online]. Available: https://www.theguardian.com/technology/2021/mar/16/google-smart-display-tracks-sleep-radar-nest-hub-second-gen

[28] P. Addabbo, M. L. Bernardi, F. Biondi, M. Cimitile, C. Clemente, and D. Orlando, "Temporal convolutional neural networks for radar micro-Doppler based gait recognition†," *Sensors*, vol. 21, no. 2, pp. 1–15, 2021, doi: 10.3390/S21020381.

[29] M. Otero, "Application of a continuous wave radar for human gait recognition," in *Proc. Signal Process. Sens. Fusion, Target Recognit.*, 2005, p. 538, doi: 10.1117/12.607176.

[30] L. Fei, H. Binke, Z. Hang, and D. Hao, "Human gait recognition using micro-Doppler features," in *Proc. 5th Global Symp. Millimeter-Waves*, 2012, pp. 326–329, doi: 10.1109/Gsmm.2012.6314067.

[31] P. Janakaraj, K. Jakkala, A. Bhuyan, Z. Sun, P. Wang, and M. Lee, "Star: Simultaneous tracking and recognition through millimeter waves and deep learning," in *Proc. 12th IFIP Wireless Mobile Netw. Conf.*, 2019, pp. 211–218, doi: 10.23919/Wmnc.2019.8881354.

[32] Q. Zou, Y. Wang, Q. Wang, Y. Zhao, and Q. Li, "Deep learning-based gait recognition using smartphones in the wild," *IEEE Trans. Inf. Forensics Security*, vol. 15, pp. 3197–3212, 2020, doi: 10.1109/TIFS.2020.2985628.

[33] P. Addabbo, M. L. Bernardi, F. Biondi, M. Cimitile, C. Clemente, and D. Orlando, "Gait recognition using FMCW radar and temporal convolutional deep neural networks," in *Proc. IEEE Int. Workshop Metrol. Aerosp. Metroaerosp.*, 2020, pp. 171–175, doi: 10.1109/Metroaerospace48742.2020.9160199.

[34] J. L. Geisheimer, W. S. Marshall, and E. Greneker, "A continuous-wave (CW) radar for gait analysis," in *Proc. Conf. Record Asilomar Conf. Signals, Syst. Comput.*, vol. 1, 2001, pp. 834–838, doi: 10.1109/Acssc.2001.987041.

[35] C. Hornsteiner and J. Detlefsen, "Characterisation of human gait using a continuous-wave radar at 24 GHz," *Adv. Radio Sci.*, vol. 6, pp. 67–70, May 2008, doi: 10.5194/Ars-6-67-2008.

[36] J. Zhang, "Basic gait analysis based on continuous wave radar," *Gait Posture*, vol. 36, no. 4, pp. 667–671, 2012, doi: 10.1016/J.Gaitpost.2012.04.020.

[37] M. G. Anderson and R. L. Rogers, "Micro-Doppler analysis of multiple frequency continuous wave radar signatures," in *Proc. Radar Sens. Technol.*, 2007, Art. no. 65470A, doi: 10.1117/12.719800.

[38] D. Tahmoush and J. Silvious, "Radar micro-Doppler for long range front-view gait recognition," in *Proc. IEEE 3rd Int. Conf. Biometr. Theory, Appl. Syst.*, 2009, pp. 1–6, doi: 10.1109/Btas.2009.5339049.

[39] A. Boroomand, G. Shaker, P. P. Morita, A. Wong, and J. Boger, "Autonomous gait speed estimation using 24GHz FMCW radar technology," in *Proc. IEEE EMBS Int. Conf. Biomed. Health Inform.*, Mar. 2018, pp. 66–69, doi: 10.1109/Bhi.2018.8333371.

[40] M. Alizadeh, H. Abedi, and G. Shaker, "Low-cost low-power in-vehicle occupant detection with mm-Wave FMCW radar," in *Proc. IEEE Sensors*, Oct. 2019, pp. 1–4, doi: 10.1109/SENSORS43011.2019.8956880.

[41] H. Abedi, S. Luo, and G. Shaker, "On the use of low-cost radars and machine learning for in-vehicle passenger monitoring," in *Proc. IEEE 20th Topical Meeting Silicon Monolithic Integr. Circuits RF Syst.*, Jan. 2020, pp. 63–65, doi: 10.1109/SIRF46766.2020.9040191.

[42] H. Abedi, S. Luo, V. Mazumdar, M. Riad, and G. Shaker, "AI-powered in-vehicle passenger monitoring using low-cost mm-Wave radar," *IEEE Access*, vol. 10, pp. 18998–19012, 2021, doi: 10.1109/ACCESS.2021.3138051.

[43] F. Quaiyum, N. Tran, J. E. Piou, O. Kilic, and A. E. Fathy, "Noncontact human gait analysis and limb joint tracking using Doppler radar," *IEEE J. Electromagn. RF Microw. Med. Biol.*, vol. 3, no. 1, pp. 61–70, Mar. 2019, doi: 10.1109/JERM.2018.2881238.

[44] H. Chen and W. Ye, "Classification of human activity based on radar signal using 1-D convolutional neural network," *IEEE Geosci. Remote Sens. Lett.*, vol. 17, no. 7, pp. 1178–1182, Mar. 2020, doi: 10.1109/LGRS.2019.2942097.

[45] J. P. Zhu, H. Q. Chen, and W. Bin Ye, "Classification of human activities based on radar signals using 1D-CNN and LSTM," in *Proc. IEEE Int. Symp. Circuits Syst.*, 2020, pp. 1–5, doi: 10.1109/ISCAS45731.2020.9181233.

[46] D. P. Fairchild and R. M. Narayanan, "Classification of human motions using empirical mode decomposition of human micro-Doppler signatures," *IET Radar, Sonar Navig.*, vol. 8, no. 5, pp. 425–434, Jun. 2014, doi: 10.1049/IET-RSN.2013.0165.

[47] X. Yang, P. Chen, M. Wang, S. Guo, C. Jia, and G. Cui, "Human motion serialization recognition with through-the-wall radar," *IEEE Access*, vol. 8, pp. 186879–186889, 2020, doi: 10.1109/Access.2020.3029247.

[48] M. Wang, G. Cui, X. Yang, and L. Kong, "Human body and limb motion recognition via stacked gated recurrent units network," *IET Radar, Sonar Navig.*, vol. 12, no. 9, pp. 1046–1051, 2018, doi: 10.1049/Iet-Rsn.2018.5054.

[49] H. Abedi et al., "Non-visual and contactless wellness monitoring for long term care facilities using mm-Wave radar sensors," in *Proc. IEEE Sensor Conf.*, 2022, pp. 1–4.

[50] P. F. Edemekong, D. L. Bomgaars, S. Sukumaran, and S. B. Levy, "Activities of daily living," in *Encyclopedia of the Neurological Sciences*. Waltham, MA, USA: Academic, Jul. 2021, pp. 47–48. Accessed: Sep. 30, 2021. [Online]. Available: https://www.ncbi.nlm.nih.gov/books/NBK470404/

[51] H. Abedi, G. Shaker, and C. Magnier, "Improving passenger safety in cars using novel radar signal processing," *Eng. Rep.*, vol. 3, no. 12, 2021, Art. no. e12413. [Online]. Available: https://doi.org/10.1002/eng2.12413

[52] "Azure machine learning documentation," Microsoft. 2021. [Online]. Available: https://learn.microsoft.com/En-Us/Azure/Machine-Learning/

[53] I. Nirmal, A. Khamis, M. Hassan, W. Hu, and X. Zhu, "Deep learning for radio-based human sensing: Recent advances and future directions," *IEEE Commun. Surveys Tuts.*, vol. 23, no. 2, pp. 995–1019, 2nd Quart., 2021.

[54] L. Deng and D. Yu, "Deep learning: Methods and applications," *Found. Trends Signal Process.*, vol. 7, nos. 3–4, pp. 197–387, 2013, doi: 10.1561/2000000039.

[55] "Single-chip 76-GHz to 81-GHz automotive radar sensor integrating MCU and hardware accelerator," AWR1443 Data Sheet, Texas Instrum., Dallas, TX, USA, 2022. [Online]. Available: https://www.ti.com/product/AWR1443

[56] "Ansys HFSS—3D high frequency simulation software." Accessed: Aug. 16, 2021. [Online]. Available: https://www.ansys.com/products/electronics/ansys-hfss

[57] M. Mercuri, I. R. Lorato, Y. H. Liu, F. Wieringa, C. van Hoof, and T. Torfs, "Vital-sign monitoring and spatial tracking of multiple people using a contactless radar-based sensor," *Nat. Electron.*, vol. 2, no. 6, pp. 252–262, Jun. 2019, doi: 10.1038/s41928-019-0258-6.

[58] M. Alizadeh, G. Shaker, J. C. M. de Almeida, P. P. Morita, and S. Safavi-Naeini, "Remote monitoring of human vital signs using mm-Wave FMCW radar," *IEEE Access*, vol. 7, pp. 54958–54968, 2019, doi: 10.1109/ACCESS.2019.2912956.

[59] C. Ammann-Reiffer, C. H. G. Bastiaenen, R. A. De Bie, and H. J. A. Van Hedel, "Measurement properties of gait-related outcomes in youth with neuromuscular diagnoses: A systematic review," *Phys. Ther.*, vol. 94, no. 8, pp. 1067–1082, Aug. 2014, doi: 10.2522/Ptj.20130299.

[60] D. N. Martini, G. C. Goulet, D. H. Gates, and S. P. Broglio, "Long-term effects of adolescent concussion history on gait, across age," *Gait Posture*, vol. 49, pp. 264–270, Sep. 2016, doi: 10.1016/J.Gaitpost.2016.06.028.

[61] "Azure IoT edge documentation." Microsoft. 2020. [Online]. Available: https://learn.microsoft.com/En-Us/Azure/Iot-Edge/?View=Iotedge-2020-11

[62] "How to capture IoT data in Azure." 2020. [Online]. Available: https://www.mssqltips.com/sqlservertip/6335/how-to-capture-iot-data-in-azure